Geophysical Journal International

Geophys. J. Int. (2014) doi: 10.1093/gji/ggt497

Geophysical Journal International Advance Access published January 3, 2014

EXPRESS LETTER

Fine-scale gas distribution in marine sediments assessed from deep-towed seismic data

S. Ker,[1] Y. Le Gonidec,[2] B. Marsset,[1] G. K. Westbrook,[1,3] D. Gibert[2,4] and T. A. Minshull[3]

[1] *IFREMER, Géosciences Marines, Centre de Brest, F-29280 Plouzané, France. E-mail: stephan.ker@ifremer.fr*
[2] *Géosciences Rennes (CNRS UMR 6118), Université Rennes 1, Bât. 15 Campus de Beaulieu, F-35042 Rennes cedex, France*
[3] *National Oceanography Centre Southampton, University of Southampton, Southampton SO14 3ZH, United Kingdom*
[4] *Institut de Physique du Globe de Paris (CNRS UMR 7154), Sorbonne Paris Cité, 1 rue Jussieu, F-75238 Paris cedex, France*

Accepted 2013 December 6. Received 2013 December 6; in original form 2013 November 6

SUMMARY

In the context of seismic imaging of gas/gas-hydrate systems, the fine-scale structure of subseabed gas-related reflections is assessed by taking advantage of the source signature of the deep-towed high-resolution SYSIF seismic device. We demonstrate the value of an original wavelet-based method and associated multiscale seismic attributes, applied to seismic data recently acquired on the western margin of the Arctic archipelago of Svalbard. From analysis in the wavelet domain, we recognize two types of gas-related reflections associated with submetre-scale distribution of gas. We identify a thin gas-charged layer associated with an apparent normal polarity reflection, and we detect gas patches associated with a reverse-polarity bright spot with frequency-dependent elastic properties at small seismic wavelengths. The results provide valuable information on the scale of features through which gas migrates and resolve ambiguities in the interpretation of the seismic data.

Key words: Wavelet transform; Gas and hydrate systems; Wave propagation; Acoustic properties; Arctic region.

1 INTRODUCTION

For many years, the seismic reflection has been the main technique for detecting the presence of shallow gas in marine sediments (Judd & Hovland 1992). The presence of gas can be detected from the enhanced amplitude and polarity reversal of seismic reflections, seismic blanking zones (Yun *et al.* 1999) and velocity pull-down (Plaza-Faverola *et al.* 2010). More quantitative geophysical characterization concerning gas saturation and volume estimation based on AVO analysis (Bunz *et al.* 2005), attenuation (Morgan *et al.* 2012) or *P*- and *S*-wave velocity inversion (Westbrook *et al.* 2008) is limited to the macroscopic scale ($\gg$1 m). To date, the seismic characterization of gas-related reflectors to reveal the nature of the distribution of gas within its host sediments at a scale of $\sim$1 m is not routinely achieved without borehole seismic techniques.

A means to efficiently investigate the gas-charged zones in more detail can be provided by recently developed high-resolution seismic systems, such as the DTAGS and the SYSIF deep-towed devices (Wood *et al.* 2008; Ker *et al.* 2010). An original multiscale seismic analysis, introduced by Le Gonidec *et al.* (2002) to characterize complex interfaces (Le Gonidec & Gibert 2007) and recently applied in geophysical imaging (Gesret *et al.* 2010), has been developed for SYSIF seismic data by Ker *et al.* (2011, 2012, 2013) to demonstrate the value of the method in characterizing the fine-scale structure of subseabed reflectors.

This new approach has been used to assess for the first time the fine-scale nature and properties of gas-charged layers in the western margin of the Arctic archipelago of Svalbard. Knowledge of the shallow distribution of gas in the upper continental slope off west Svalbard (Fig. 1a; Sarkar *et al.* 2012) is crucial to understand the relationship between the occurrence of subseabed gas-hydrate and hundreds of gas seeps from the seabed observed in 2008 (Westbrook *et al.* 2009). Seismic reflection data show that the area in which the seeps occur is layered, with a complex stratigraphy. Seismic bright spots of reverse polarity, to a large degree, lie along particular reflectors, indicating that gas migration and, by inference, the distribution of hydrate exhibit stratigraphic control. It is not possible from visual examination of the seismic sections to judge the thickness of the gas-charged zones, nor to define the distribution of the free gas within them. Furthermore, high-amplitude reflectors of apparently normal polarity occur locally, in association with the reverse-polarity reflectors. These might be produced by strong concentrations of hydrate, by authigenic carbonate or by interference between reflections from the boundaries of gas-charged bodies. To resolve some of the questions, of interpretation of the seismic data, we applied the multiscale seismic analysis to high-resolution SYSIF

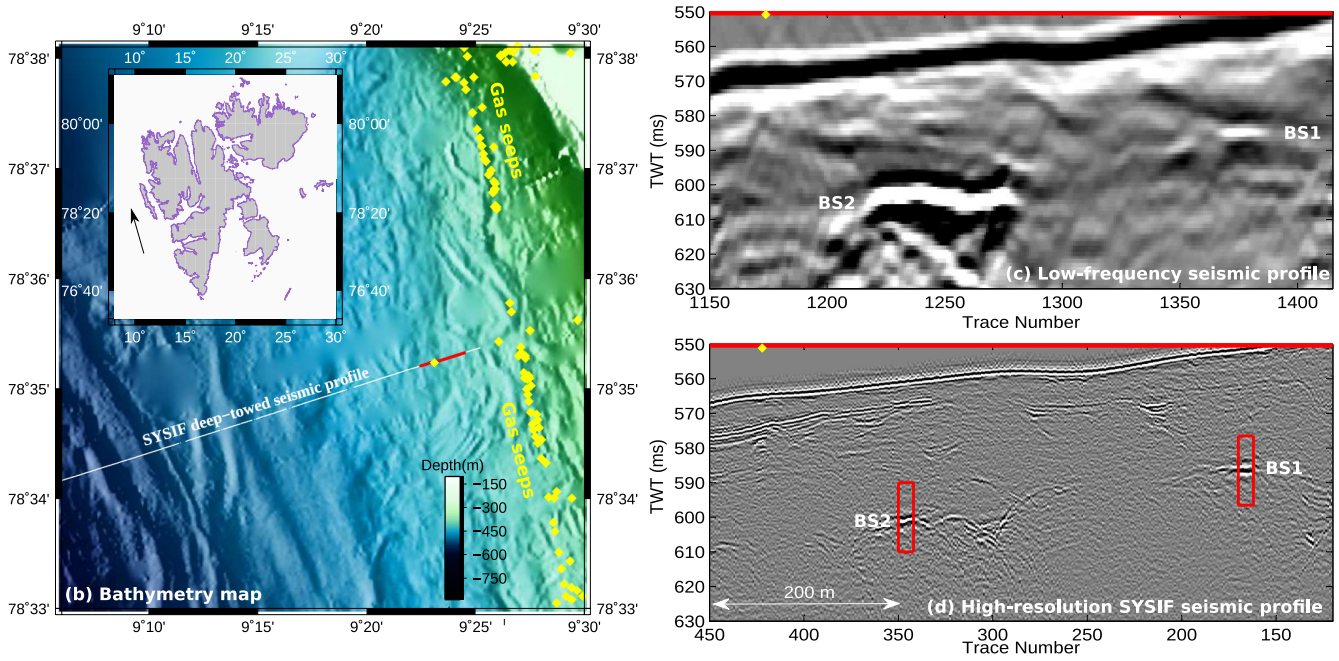

Figure 1. (a) Geographical location, shown by the black arrow and (b) bathymetric map of the study area, offshore Svalbard, in which there are numerous gas seeps (Westbrook *et al.* 2009). (c) Low-frequency seismic profile, shown in (a) by the red line, acquired in 2008 with an air-gun seismic source (30–150 Hz). Two bright-spot reflections located by the red boxes (BS1 and BS2) have been interpreted as gas-charged layers. (d) High-frequency seismic profile at the same location acquired in 2011 with the SYSIF deep-towed seismic device (220–1050 Hz).

seismic data that have been acquired in the same area (Fig. 1d) in 2011 to investigate the gas-charged layers in more detail.

2 MULTISCALE SEISMIC ANALYSIS BASED ON THE WAVELET RESPONSE

The wavelet response (WR) method (Le Gonidec *et al.* 2002) employs a multiscale sounding of the medium with source signals $a^{-1}\xi(t/a)$ forming a wavelet family. ξ is a short-time source signal (e.g. a Ricker wavelet) whose wavelength is controlled by the dilation factor $a > 0$. The collection of seismic traces so obtained constitutes the WR of the medium:

$$R\,[\xi,\,p]\,(t,a) = a^{-1}\,(\xi(t/a) \otimes p)\,(t)\,, \tag{1a}$$

$$= a^{-1}\,(\xi(t/a) * r)\,(t)\,. \tag{1b}$$

In eq. (1a), $\otimes$ represents the wavelet propagation through the medium with acoustic impedance $p(z)$. Introducing the reflectivity $r(t)$ of the medium, the WR can be rewritten as eq. (1b), where $*$ represents time convolution, recognized as a continuous wavelet transform (CWT) whose properties are shared by the WR (Le Gonidec *et al.* 2002). In particular, the capability of the CWT to characterize abrupt changes in signals from the so-called ridge functions, which represent the variations of the CWT amplitude as a function of dilation a (Mallat & Hwang 1992), may be exploited with the WR to study the fine structure of seismic reflectors. For instance, a reflector corresponding to a homogeneous discontinuity has a linear ridge function in a log−log diagram, with a slope α equal to its regularity (e.g. -1 for an infinitely thin layer and 0 for a step-like reflector).

Following this approach, Ker *et al.* (2011) introduced new multiscale seismic attributes based on the CWT properties and Ker *et al.* (2012 and 2013) developed a wavelet-based processing to establish a rigorous equivalence with the WR when using limited frequency bandwidth seismic sources. This source-corrected method takes advantage of deep-towed seismic sources, characterized by low noise levels, large frequency bandwidths and source signatures measurements. These previous works demonstrated the efficiency of the method in assessing the inner fine-scale structure of complex reflectors with the deep-towed SYSIF device (Ker *et al.* 2010) and the approach is now performed for gas-charged layers.

3 GAS-CHARGED LAYERS IMAGED BY HIGH-FREQUENCY SEISMIC DATA

The presence of gas in the upper continental slope offshore Svalbard (Fig. 1a) was previously identified on seismic sections (Sarkar *et al.* 2012) from a survey employing a 96-channel hydrophone streamer and mini-GI (generator-injector) air guns to provide data with a low-frequency (LF) range of 30–150 Hz. The processing of the LF seismic data, including prestack migration, yielded vertical and lateral resolutions of 4 and 15 m, respectively. A segment of a seismic profile, located by the red line in the bathymetry map of Fig. 1(b), highlights two of many bright-spots, BS1 and BS2 (Fig. 1c). These features are characterized by both reverse polarity and significant seismic reflection strength, and have been interpreted to be caused by free gas (Sarkar *et al.* 2012).

The same area has recently been surveyed with the high-frequency (HF) SYSIF system. The seismic source is a Janus-Helmholtz transducer, which transmits a Chirp signal in the HF bandwidth of 220–1050 Hz, and the receiver is a single hydrophone. The seismic data processing involves a correction of the immersion depth of the SYSIF, a source signature deconvolution described in Ker *et al.* (2010), and a Stolt migration. The vertical and lateral resolutions of the HF system are 1 and 3 m, respectively. The track of the HF line lies within the radius of the first Fresnel zone at the seabed of the LF data. The SYSIF seismic imaging of BS1 and BS2 (Fig. 1d) shows significant differences compared with the LF seismic profile, which are used to develop a more detailed interpretation.

4 NORMAL POLARITY RELATED TO THE THIN GAS-CHARGED LAYER BS1

The gas-related seismic reflection BS1, identified with an apparent reverse polarity in the LF seismic profile, shows unexpectedly a normal polarity in the SYSIF seismic profile. Taking advantage of the SYSIF source signature, we determine the source-corrected WR of BS1 (Fig. 2a) to characterize its complex structure. Following the optimal processing developed by Ker *et al.* (2013), the effective analysing wavelet associated with the SYSIF source is a fifth Gaussian derivative function, an odd wavelet with six extrema. However, the coherent cone-like structure of the source-corrected WR has one more extremum (the first and last extrema are too weak to be visible in Fig. 2a), indicating the Dirac discontinuity of an infinitely thin layer (Le Gonidec *et al.* 2002). Furthermore, the multiscale seismic attribute of BS1 based on the central extremum ridge function (Fig. 2b, black crosses) is not linear but shows a maximum at $\ln a_c = -6.1$ [the uncertainty on the critical dilation a_c is discussed in (Ker *et al.* 2011)]. This observation suggests that BS1 is a thin layer of thickness $e = a_c V_p/4$ (Ker *et al.* 2013). With a *P*-wave velocity V_p of around 1300 m s^{-1} (Sarkar *et al.* 2012), the layer thickness is 70 ± 10 cm, that is the internal structure can now be resolved at submetric scale.

To reinforce this analysis, we compute the source-corrected WRs for two synthetic thin layers, both with the same two-way traveltime thickness but with different sound speeds in each layer (Fig. 2c). The slower (upper) and faster (lower) layer models could represent gas-charged and carbonate layers, respectively. The multiscale analysis of the former model, including the source-corrected WR (Fig. 2d, top) and ridge function (Fig. 2b, red curve), is in very good agreement with that of BS1 (Figs 2a and b, respectively), that is BS1 is actually equivalent to a gas-charged layer. The shapes of both ridge functions are similar and show a maximum associated with the transition between the large and fine-scale appearances of the reflector, that is with interactions between the wavelets and the inner structure of BS1. Note that the synthetic WR is provided to illustrate the multiscale analysis efficiency in deriving directly the fine-scale structure, but the result comes independently from the information shown in Figs 2(a) and (b).

As a consequence, while the HF seismic image of BS1 would not be conventionally interpreted to be caused by gas, the SYSIF source-corrected WR demonstrates that the apparent normal polarity observed for BS1 is produced by the presence of gas locally trapped in a thin layer.

5 HETEROGENEOUS NATURE OF THE GAS-CHARGED MEDIUM BS2

In the LF seismic profile (Fig. 1c), the waveform of the bright spot BS2 is similar to that of the seafloor reflection, but with an inverse polarity, that is BS2 is interpreted as the top interface of a gas-charged layer (Sarkar *et al.* 2012), with no significant attenuation in this LF range. In the HF seismic profile, the waveform of BS2 is also characterized by an inverse polarity but its frequency spectrum is shifted towards the lower frequencies when comparing to the frequency spectra of both the seismic reflection at the seabed and in the medium overlying BS2. There is no significant attenuation in the medium overlying BS2, for which the frequency spectrum of the reflected wavelet is thus more likely to be related to the physical properties of the underlying medium.

To develop the interpretation further and to assess the characteristic size of the gas distribution, we perform the source-corrected WR of BS2 (Fig. 3a), following the wavelet-based processing described above, and extract the main ridge function (Fig. 3b, black crosses). The WR is a single coherent cone-like structure with same number of extrema as in the effective analysing wavelet. In the framework of the WR properties (Le Gonidec *et al.* 2002), this

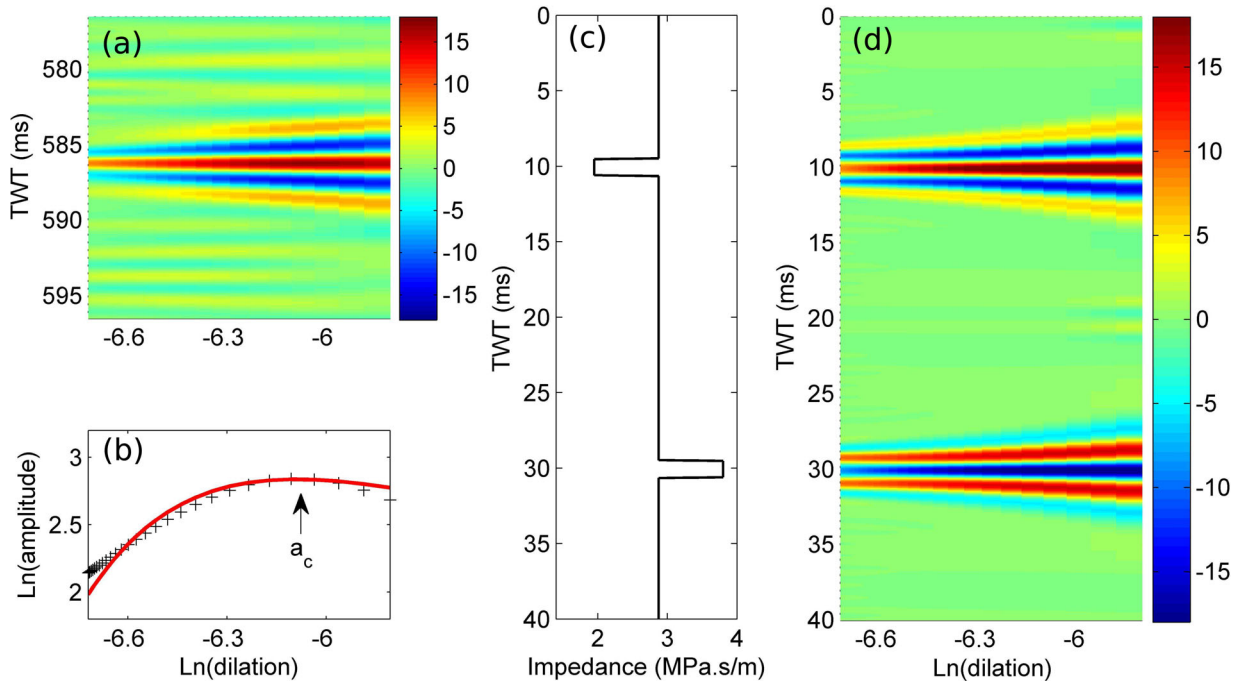

Figure 2. (a) Source-corrected WR of BS1, (b) ridge functions of BS1 and of the synthetic thin layer (stars and red curve, respectively). (c) and (d) Synthetic impedance profile in the TWT domain of two different homogeneous thin layers (70 and 107 cm, respectively) and associated WR, respectively. The top layer represents a gas-charged layer with a *P*-wave velocity $V_p = 1300$ m s^{-1} and a density $\rho = 1500$ kg m^{-3}, and the bottom layer represents a carbonate layer with $V_p = 2000$ m s^{-1} and $\rho = 1800$ kg m^{-3}.

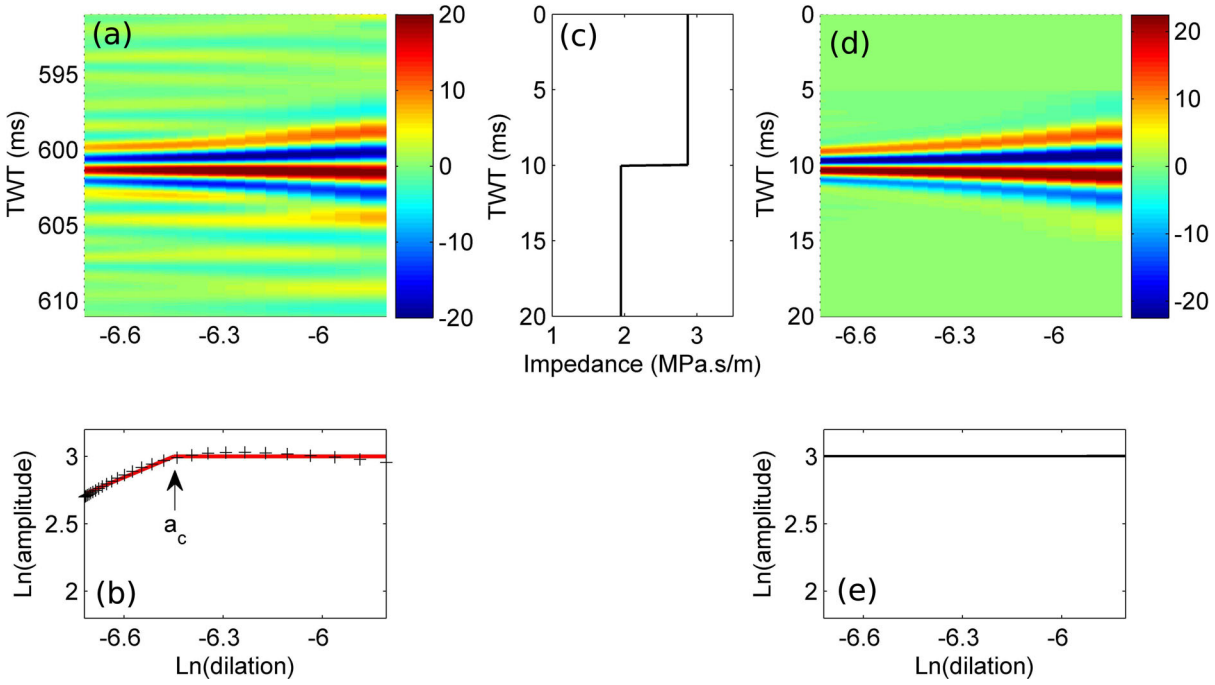

Figure 3. (a) and (b) Source-corrected WR and ridge function of BS2, respectively. The ridge function (stars) is approximated by two segments (red lines). (c) Synthetic impedance profile of a homogeneous half-space medium (Heaviside-like discontinuity). (d) and e) Theoretical WR and ridge function, respectively.

observation indicates that the interface is equivalent to a step-like discontinuity at which seismic waves are reflected (Fig. 3c). The source-corrected WR is in very good agreement with the theoretical WR of such a homogeneous discontinuity (Fig. 3d), for which the theoretical ridge function is a horizontal line $\alpha = 0$ (Fig. 3e). Accordingly, the ridge function of BS2 (Fig. 3b) is nearly flat at large dilations ($\alpha \simeq 0$ for $a > a_c$), and the observed weak perturbations can be attributed to surrounding reflectors. However, a noticeable decrease of the amplitude is observed at smaller dilations ($\alpha \simeq 1$ for $a < a_c$), where the wavelets respond to the small-scale properties of the lower medium associated with BS2. The approximation of the ridge function with straight lines (Fig. 3b) locates the critical dilation a_c at $\ln a_c = -6.45$. Depending on the wavelength λ of the seismic source, the lower medium shows two distinct behaviours with a transition at $\lambda_c = V_p a_c \simeq 2$ m: a quasi-static seismic response for $\lambda > \lambda_c$ (Rayleigh scattering), in the sense that the elastic properties do not depend on the seismic frequency, or a dynamic response for $\lambda < \lambda_c$, where heterogeneities much smaller than λ_c induce multiple scattering of the seismic waves. Accordingly, the BS2 waveform corresponds to the seismic reflection at the interface between an overlying, non-dissipative homogeneous medium and an underlying, heterogeneous gas-charged medium with submetre-scale distribution of gas.

6 DISCUSSION AND CONCLUSION

The SYSIF source-corrected WR of the bright spot BS1, identified as a gas-charged layer in the LF seismic profile, reveals that the normal-polarity of BS1 can be explained by acoustic wave interactions within a homogeneous gas-charged layer that is less than 1-m thick. A conventional interpretation would have associated the normal-polarity reflector with an interface underlain by a sediment layer with high acoustic impedance, such as hydrate or authigenic carbonate, but not consistent with the reverse polarity of the LF reflection. Thus, one is led to speculate that a small gas-charged body with sharp boundaries produces the SYSIF response of BS1, and may lie within a more amorphous zone of gas, that is a non-uniform and with lower gas concentration, which produces the LF response. The limited lateral extent of BS1 as imaged by SYSIF and small thickness do not allow the LF data, which have a much wider Fresnel zone and a lower resolution, to detect the small body or the detailed nature of the gas-distribution of BS1.

The wavelet-based method reveals that the bright spot BS2 corresponds to the top interface of a complex medium with a heterogeneous distribution of gas-patches. Such multiscale behaviour has already been observed for a granular medium (Le Gonidec & Gibert 2007), homogeneous at large scale in agreement with quasi-static effective medium theories and presenting frequency-dependent elastic properties at smaller scale in agreement with dynamic effective medium theories that take into account scattering regime. The transition between these two effective behaviours occurs at $\lambda = 2\pi d$, where d is the size of the inclusions. Thus, BS2 is likely to be caused by a patchy gas distribution whose characteristic dimension is $d \simeq \lambda_c/6$ ($\simeq$30 cm), that is submetric sized gas heterogeneities.

We have shown that the complex structure and properties of gas-related seismic reflectors at a small scale can be identified, and their interpretation can be improved greatly, with the source-corrected WR method, which utilises the source signature of the SYSIF high-resolution deep-towed seismic device. The results of the application of the method to seismic reflection data from offshore Svalbard provide valuable information on the scale of features through which gas migrates and resolve ambiguities in the interpretation of the data that might, otherwise lead to incorrect geological hypotheses being proposed for the nature of the subseabed gas system.

ACKNOWLEDGEMENTS

Data acquisition was partially supported by UK Natural Environment Research Council grants NE/H002732/1 and NE/H022260/1. This is IPGP contribution number 3465.

REFERENCES

Bunz, S., Mienert, J., Vanneste, M. & Andreassen, K., 2005. Gas hydrates at the Storegga Slide: constraints from an analysis of multi-component, wide-angle seismic data, *Geophysics,* **70,** B19–B34.

Gesret, A., Laigle, M., Diaz, J., Sachpazi, M. & Hirn, A., 2010. The oceanic nature of the African slab subducted under Peloponnesus: thin-layer resolution from multiscale analysis of teleseismic P-to-S converted waves, *Geophys. J. Int.,* **183,** 833–849.

Judd, A.G. & Hovland, M., 1992. The evidence of shallow gas in marine sediments, *Cont. Shelf Res.,* **12,** 1081–1095.

Ker, S., Marsset, B., Garziglia, S., Le Gonidec, Y., Gibert, D., Voisset, M. & Adamy, J., 2010. High-resolution seismic imaging in deep sea from a joint deep-towed/OBH reection experiment: application to a Mass Transport Complex offshore Nigeria, *Geophys. J. Int.,* **182,** 1524–1542.

Ker, S., Le Gonidec, Y., Gibert, D. & Marsset, B., 2011. Multiscale seismic attributes: a wavelet-based method and its application to high-resolution seismic and ground truth data, *Geophys. J. Int.,* **187,** 1038–1054.

Ker, S., Le Gonidec, Y. & Gibert, D., 2012. Multiscale seismic attributes: source-corrected wavelet response and application to high-resolution seismic data, *Geophys. J. Int.,* **190,** 1746–1760.

Ker, S., Le Gonidec, Y. & Gibert, D., 2013. Multiresolution seismic data fusion with a generalized wavelet-based method to derive subseabed acoustic properties, *Geophys. J. Int.,* **195,** 1370–1383.

Le Gonidec, Y., Gibert, D. & Proust, J.-N., 2002. Multiscale analysis of waves reflected by complex interfaces: basic principles and experiments, *J. geophys. Res.,* **107**(B9), 2184.

Le Gonidec, Y. & Gibert, D., 2007. Multiscale analysis of waves reflected by granular media: acoustic experiments on glass beads and effective medium theories, *J. geophys. Res.,* **112,** B05103, doi:10.1029/2006JB004518.

Mallat, S. & Hwang, W.L., 1992. Singularity detection and processing with wavelets, *IEEE Trans. Inf. Theory,* **38,** 617–643.

Morgan, E.C., Vanneste, M., Lecomte, I., Baise, L.G., Longva, O. & McAdoo, B., 2012. Estimation of free gas saturation from seismic reflection surveys by the genetic algorithm inversion of a P-wave attenuation model, *Geophysics,* **77,** R175–R187.

Plaza-Faverola, A., Westbrook, G.K., Ker, S., Exley, R.J.K., Gailler, A., Minshull, T.A. & Broto, K., 2010. Evidence from 3D seismic tomography for a substantial accumulation of gas hydrate in a fluid-escape chimney in the Nyegga pockmark field, offshore Norway, *J. geophys. Res.,* **115,** B08104, doi:10.1029/2009JB007078.

Sarkar, S. *et al.*, 2012. Seismic evidence for shallow gas-escape features associated with a retreating gas hydrate zone offshore west Svalbard, *J. geophys. Res.,* **117**(B9), B09102, doi:10.1029/2011JB009126.

Westbrook, G.K. *et al.*, 2008. Estimation of gas hydrate concentration from multi-component seismic data at sites on the continental margins of NW Svalbard and the Storegga region of Norway, *Mar. Pet. Geol.,* **25,** 744–758.

Westbrook, G.K. *et al.*, 2009. Escape of methane gas from the seabed along the West Spitsbergen continental margin, *Geophys. Res. Lett.,* **36,** L15608, doi:10.1029/2009GL039191.

Wood, W., Hart, P., Hutchinson, D., Dutta, N., Snyder, F., Coffin, R. & Gettrust, J., 2008. Gas and gas hydrate distribution around seafloor seeps in Mississipi Canyon, Nothern Gulf of Mexico, using multi-resolution seismic imagery, *Mar. Petrol. Geol.,* **25,** 952–959.

Yun, J.W., Orange, D.L. & Field, M.E., 1999. Subsurface gas offshore of northern California and its link to submarine geology, *Mar. Geol.,* **154,** 357–368.